Journal of Statistical Physics, Vol. 46, Nos. 1/2, 1987

Equilibrium Polymerization in a Solvent: Solution on the Bethe Lattice

Jürgen F. Stilck[1,2] **and John C. Wheeler**[1]

Received August 27, 1986

The lattice model for equilibrium polymerization in a solvent proposed by Wheeler and Pfeuty is solved exactly on a Bethe lattice (core of a Caylay tree) with general coordination number q. Earlier mean-field results are reobtained in the limit $q \to \infty$, but the phase diagrams show deviations from them for finite q. When $q = 2$, our results turn into the solution of the one-dimensional problem. Although the model is solved directly, without the use of the correspondence between the equilibrium polymerization model and the dilute $n \to 0$ model, we verified that the latter model may also be solved on the Bethe lattice, its solution being identical to the direct solution in all parameter space. As observed in earlier studies of the pure $n \to 0$ vector model, the free energy is not always convex. We obtain the region of negative susceptibility for our solution and compare this result with mean field and renormalization group (ε-expansion) calculations.

KEY WORDS: Equilibrium polymerization; polymers; $n \to 0$ vector model; Bethe lattice; Cayley tree phase transitions; critical phenomena; magnetism.

1. INTRODUCTION

The recognition that the problems of equilibrium polymerization[1a,1b] and equilibrium polymerization in a solvent[2a,2b] can be mapped into the $n \to 0$ limit of a pure or dilute n-vector model of magnetism, following pioneering work by De Gennes[3] and Des Cloizeaux,[4] has made it possible to study these problems from the point of view of the modern theory of critical phenomena, which is well established for magnetic systems. It is par-

[1] Department of Chemistry, University of California-San Diego, La Jola, California 92093.
[2] Permanent Address: Instituto de Física, Universidade de São Paulo, 01498, São Paulo, SP, Brazil.

0022-4715/87/0100-0001$05.00/0

ticularly useful to explore this analogy because the symmetries in the magnetic systems are usually much more visible than in their polymeric counterparts. It is remarkable that mean-field calculations for the magnetic models become identical with the earlier theories of Gee[5] and Tobolsky and Eisenberg[6] for pure sulfur and Scott[7] for sulfur solutions, probably the most studied physical realizations of equilibrium polymerization in the absence and presence of a solvent. The symmetry of the underlying magnet allowed the lower critical solution temperature in Scott's theory to be identified as a tricritical point in the corresponding magnet. In addition, the analogy between magnetic and polymeric models allowed the application of techniques of the modern theory of critical phenomena, well established for magnetic systems, to the study of polymerization. The use of nonclassical critical exponents from the magnetic theory has resulted in improved descriptions of the anomalies in the heat capacity,[1a,8] density,[9] and dielectric constant[10] of pure sulfur and the fraction of polymerized material in sulfur[1a,8] and polytetrahydrofuran.[11] For a recent review on the experimental situation in this field we refer to the article by Knobler and Scott.[12]

In this paper we examine a different kind of systematic improvement on the mean field approximation to the magnet and to the equivalent Gee[5]–Tobolsky–Eisenberg[6] theory. We solve the problems of equilibrium polymerization and equilibrium polymerization in a solvent on the Bethe lattice, that is, we study the behavior of the model on sites deep inside a Cayley tree with general coordination number q. Although it is possible to study the model on a complete Cayley tree, it is expected that the results for that case will be qualitatively different from the ones observed on lattices with translation invariance,[13] due to the nonnegligible effects of the surface sites, even in the thermodynamic limit, in the Cayley tree. In the so-called Bethe lattice calculations the model is defined on the Cayley tree, but only contributions from sites in the core of the tree are considered. For the nearest neighbor Ising model, the Bethe–Peierls approximation on a regular Bravais lattice with the same coordination number is recovered.[14] Our approach is quite similar to the one presented for the Ising model by Baxter.[15]

Although our solution for the equilibrium polymerization in a solvent is direct, without the use of the analogy with the corresponding magnetic model, we show in Section 6 that the solution of the dilute $n \to 0$ vector model leads to precisely the same results. Recently, it was suggested that the mapping between the two models in the absence of a solvent should break down in the low-temperature region[16] and that the polymeric system should display a "collapsed" phase in this region. We have shown elsewhere[17] that, at least to first order in the ε expansion, there is no

evidence of such a phenomenon. We see no evidence for such a breakdown here either. The identity between the direct solution of the polymeric problem on the Bethe lattice and the solution of the corresponding $n \to 0$ vector model on the same lattice is valid in all field-variable space, as may be verified by comparing the results of Sections 3 and 6.

There are two limits where our solution may be compared with earlier results. In the limit of infinite coordination number, we recover the results of the mean-field approximation to the model,[1a,1b,2a,2b,5-7] whereas when the coordination number is equal to two, our solution is the exact solution of the one-dimensional model, which was already thoroughly studied in the case of equilibrium polymerization in the absence of a solvent.[18] In general, Bethe lattice solutions seem to reduce to the man-field solutions in the limit $q \to \infty$ for models with nearest neighbor interactions only, as may be verified explicitly for the Ising model,[19] the Blume–Emery–Griffiths model[20] (dilute $n = 1$ model), and the present model. [For models with interactions beyond first neighbors, like the ANNNI model,[21] the corresponding model on the Cayley tree is not uniquely defined and the appropriate $q \to \infty$ limit may be different from the mean-field solution.] Also, we compare our result with a calculation by Gujrati,[22] which corresponds to the solution of the model in the absence of a solvent on the $q = 3$ Bethe lattice.

In Section 2 we give a brief definition of the model. A more detailed description may be found in Refs. 2a and 2b. The direct solution of the model on the Bethe lattice is presented in Section 3, in terms of a two-dimensional mapping. Also, we obtain expressions for the relevant densities and look at the solutions in the various limiting situations. We consider in some detail the particular case when no solvent is present in Section 4, and compare our results with the ones obtained by Gujrati[22] for $q = 3$. Phase diagrams are obtained and presented in Section 5 for the general model, and the effect of finite coordination number is apparent in the comparison of these phase diagrams with the man-field results. It should be stressed that, from the point of view of critical exponents, the Bethe lattice solution is obviously classical. In Section 6, we solve the dilute $n \to 0$ vector model, which corresponds to the model for equilibrium polymerization in a solvent on the Bethe lattice. We find that this solution is identical to the direct one throughout all of the parameter space, no breakdown of the analogy between models being observed.

We also examine there the locus on which the susceptibility χ of the $n \to 0$ vector model on the Bethe lattice vanishes, and find that its behavior with the coordination number q is consistent with a recent conjecture concerning the shape of this locus for the $n \to 0$ vector model on translationally invariant lattices. We also show how the shape of this locus in mean-field

theory passes continuously to the quite different shape found in the exact solution of the model in one dimension. A bief discussion of our results is given in Section 7.

2. DEFINITION OF THE MODEL

We consider a model for equilibrium polymerization in a solvent defined on a lattice that was proposed by Wheeler and Pfeuty[2a,2b] to discuss equilibrium polymerization in sulfur and is identical, in the mean-field approximation, to the earlier theory of Scott.[7]

The configuration of the lattice is defined as follows: Each site may be occupied either by a solvent molecule ($v_i = 0$) or by a monomer ($v_i = 1$). The monomers may be in two states, active or inactive, and active monomers in first-neighbor sites may connect, thus forming chain polymers. In the particular case of sulfur solutions the monomers are S_8 rings, which may be open (active) or closed (inactive). The interaction energy between first neighbors will be given by E_{00}, E_{01}, and E_{11} for solvent–solvent, solvent–monomer, and monomer–monomer pairs, respectively. The statistical weight of a chain polymer with m sites ($m-1$ bonds) is given by

$$\begin{aligned} &K_1 && \text{if} \quad m = 1 \\ &2K_1(K_p')^{m-1} && \text{if} \quad m > 1 \end{aligned} \tag{2.1}$$

The partition function for this model will be

$$\begin{aligned} Y = \sum_{\{v_i\}} \sum_{N_p} \sum_{N_b} \sum_{N_1} &\exp[-(E_{00}N_{00} + E_{01}N_{01} + E_{11}N_{11})/kT] \\ &\times [\exp(\mu_1 - \mu_0)/kT]^{\sum_i v_i} (2K_1)^{N_p} (K_p')^{N_b} (1/2)^{N_1} \Gamma(N_p, N_b, N_1, N; \{v_i\}) \end{aligned} \tag{2.2}$$

The sum $\sum_{\{v_i\}}$ is over all site configurations ($v_i = 0$ or $v_i = 1$ on each site), and N_{00}, N_{01}, and N_{11} are numbers of nearest neighbor solvent–solvent, solvent–monomer, and monomer–monomer pairs, respectively, for a given site configuration. $\Gamma(N_p, N_b, N_1, N; \{v_i\})$ stands for the number of distinguishable ways of placing N_p polymers containing a total number N_b of bonds, N_1 of which are one-site polymers, on the N-site lattice for a given site configuration $\{v_i\}$. The quantities μ_i and μ_0 are the chemical potentials for monomers and solvent molecules, respectively. One may think of $(2K_1)^{1/2}$ as playing the role of an "activity" of a polymer end and K_p' as playing the role of a statistical weight or activity for bonds. Both K_1 and K_p' contain a factor accounting for the number of ways to arrange the

polyatomic "monomer" unit within a cell. The factor $(1/2)^{N_1}$ arises because for single-cell polymers there are configurations that differ only in that the ends of the monomer are interchanged.

3. DIRECT SOLUTION OF THE MODEL ON THE BETHE LATTICE

As in Baxter's[15] solution for the Ising model on the Bethe lattice, we consider a Cayley tree with coordination number q and M generations (see Fig. 1) built by attaching q rooted subtrees of M generations to a central site. We then proceed to find recursion relations for the partial partition functions of subsequent generations. The subtrees will be classified into three categories, according to the configuration of their root (full dots stand for solute molecules and empty ones for solvent molecules)

b: occupied bond on root

u_0: unoccupied bond on root, solvent on site

u_1: unoccupied bond on root, monomer on site

Let $g_M(c)$ be the partial partition function of an M-generation subtree, which is the sum (2.2) for all configurations of the subtree compatible with a given root configuration $c(b, u_0 \text{ or } u_1)$. Figure 2 depicts how an $(M+1)$-generation subtree may be built by attaching $q-1$ of the M-generation subtrees to a new root site and bond. This process leads to the following recursion relations for the partial partition functions of the subtrees:

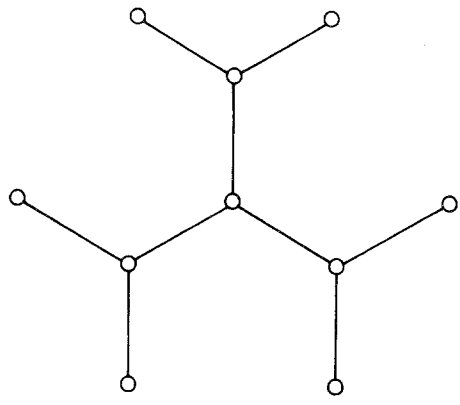

Fig. 1. A Cayley tree with $q=3$ and $M=2$ generations.

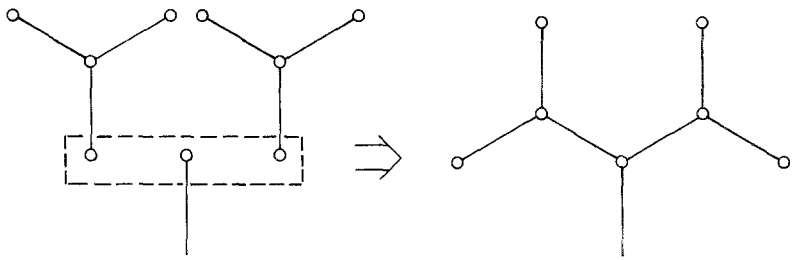

Fig. 2. Construction of a ($q=3$, $M=3$) subtree from two ($q=3$, $M=2$) subtrees.

$$
\begin{aligned}
g_{M+1}(b) &= \omega_1(2K_1K_p')^{1/2}[\omega_{01}\, g_M(u_0) + \omega_{11}\, g_M(u_1)]^{q-1} \\
&\quad + (q-1)\,\omega_{11}\omega_1 K_p'\, g_M(b)[\omega_{01}\, g_M(u_0) + \omega_{11}\, g_M(u_1)]^{q-2} \\
g_{M+1}(u_0) &= [\omega_{00}\, g_M(u_0) + \omega_{01}\, g_M(u_1)]^{q-1} \\
g_{M+1}(u_1) &= \omega_1(1+K_1)[\omega_{01}\, g_M(u_0) + \omega_{11}\, g_M(u_1)]^{q-1} \\
&\quad + (q-1)\,\omega_{11}\omega_1(2K_1K_p')^{1/2}\, g_M(b) \\
&\quad \times [\omega_{01}\, g_M(u_0) + \omega_{11}\, g_M(u_1)]^{q-2} \\
&\quad + \tfrac{1}{2}(q-1)(q-2)\,\omega_{11}^2\omega_1 K_p'\, g_M^2(b) \\
&\quad \times [\omega_{01}\, g_M(u_0) + \omega_{11}\, g_M(u_1)]^{q-3}
\end{aligned}
\tag{3.1}
$$

where

$$
\begin{aligned}
\omega_1 &= \exp[(\mu_1 - \mu_0)/kT] \\
\omega_{i,j} &= \exp(-E_{ij}/kT), \qquad i, j = 0, 1
\end{aligned}
\tag{3.2}
$$

The factor ω_1 in $g_{M+1}(b)$ and $g_{M+1}(u_1)$ accounts for the fact that a monomer rather than a solvent occupies the site. For $g_{M+1}(u_0)$, the fact that the site is occupied by a solvent and that (therefore) the bond is empty means that each of the $q-1$ M-generation subtrees above it must be either occupied by a solvent [contributing $\omega_{00}\, g_M(u_0)$] or by a monomer that does not bond to it [contributing $\omega_{01}\, g_M(u_1)$]. For $g_{M+1}(b)$, the first term accounts for the various ways in which a chain may start at the $(M+1)$th generation and the second with the number of ways in which it may continue from above. For $g_{M+1}(u_1)$ the first term accounts for the ways of obtaining an isolated monomer at the $(M+1)$th generation, the second with the ways of terminating a chain at the $(M+1)$th generation, and the third with the ways in which a chain may pass through the $(M+1)$th generation site joining the M-generation subtrees.

It is convenient to define the quantities

$$R_M = \frac{(K_p')^{1/2}\, g_M(b)}{g_M(u_1)}, \qquad S_M = \frac{\omega_{00}}{\omega_{01}} \frac{g_M(u_0)}{g_M(u_1)} \tag{3.3}$$

and the parameters

$$\begin{aligned} \omega_{\tilde{K}} &\equiv \exp[(2E_{01} - E_{00} - E_{11})/kT] = \omega_{00}\omega_{11}/\omega_{01}^2 = \exp \tilde{K} \\ \omega_{\tilde{\Delta}} &\equiv \exp\{[\mu_1 - \mu_0 - q(E_{01} - E_{00})]/kT\} = \omega_1(\omega_{01}/\omega_{00})^q = \exp \tilde{\Delta} \end{aligned} \tag{3.4}$$

The recursion relations for R_M and S_M may then be obtained from (3.1) and are given by

$$\begin{aligned} R_{M+1} = {} & \{(2K_1)^{1/2} K_p'[S_M + \omega_{\tilde{K}}]^{q-1} + (q-1)\,\omega_{\tilde{K}} K_p' R_M [S_M + \omega_{\tilde{K}}]^{q-2}\} \\ & \times \{(1+K_1)[S_M + \omega_{\tilde{K}}]^{q-1} \\ & + (q-1)\,\omega_{\tilde{K}}(2K_1)^{1/2} R_M [S_M + \omega_{\tilde{K}}]^{q-2} \\ & + \tfrac{1}{2}(q-1)(q-2)\,\omega_{\tilde{K}}^2 R_M^2 [S_M + \omega_{\tilde{K}}]^{q-3}\}^{-1} \\ S_{M+1} = {} & [S_M + 1]^{q-1} \\ & \times (\omega_{\tilde{\Delta}}\{(1+K_1)[S_M + \omega_{\tilde{K}}]^{q-1} \\ & + (q-1)\,\omega_{\tilde{K}}(2K_1)^{1/2} R_M [S_M + \omega_{\tilde{K}}]^{q-2} \\ & + \tfrac{1}{2}(q-1)(q-2)\,\omega_{\tilde{K}}^2 R_M^2 [S_M + \omega_{\tilde{K}}]^{q-3}\})^{-1} \end{aligned} \tag{3.5}$$

Examination of the exact solution for $M = 1$ reveals that the appropriate initial conditions are

$$R_0 = 0, \qquad S_0 = \frac{1 - \omega_{\tilde{K}}}{1 - \omega_{00}/\omega_{01}} \tag{3.6}$$

The partition function for the model on the M-generation Cayley tree is obtained by considering the operation of attaching q subtrees to the same central site. This leads to

$$\begin{aligned} Y_M = {} & [\omega_{00}\, g_M(u_0) + \omega_{01}\, g_M(u_1)]^q + \omega_1(1+K_1)[\omega_{01}\, g_M(u_0) + \omega_{11}\, g_M(u_1)]^q \\ & + q\omega_1(2K_1K_p')^{1/2}\,\omega_{11}\, g_M(b)[\omega_{01}\, g_M(u_0) + \omega_{11}\, g_M(u_1)]^{q-1} \\ & + \tfrac{1}{2}q(q-1)\,\omega_1 K_p'\omega_{11}^2\, g_M^2(b)[\omega_{01}\, g_M(u_0) + \omega_{11}\, g_M(u_1)]^{q-2} \end{aligned} \tag{3.7}$$

The origin of each term in the partition function is shown graphically in Fig. 3 for a Cayley tree with $q = 6$.

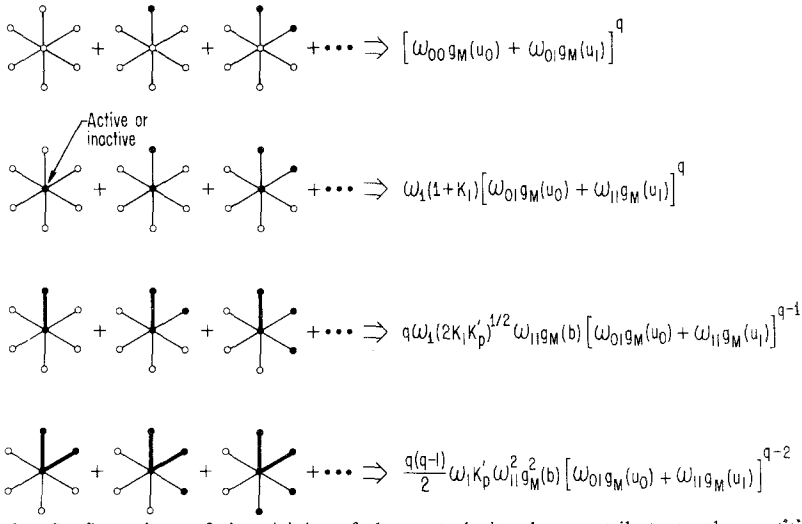

Fig. 3. Configurations of the vicinity of the central site that contribute to the partition function. (●) Solute molecules, (○) solvent molecules; heavy lines are occupied by bonds.

Now the thermodynamic properties of the model on the complete Cayley tree may be obtained from the partition function (3.7) after performing the thermodynamic limit $M \to \infty$. As was stressed in the introduction, however, the properties of the model on the Cayley tree are expected to be qualitatively different from those on lattices with translation invariance. So, following the usual procedure,[13-15] we will concentrate our attention on the behavior of the model deep inside the tree, where all sites have the same coordination number q. The quantities R_M and S_M will approach a fixed point R and S in the limit $M \to \infty$, and we will be interested in the thermodynamic properties of the model in this limit. Looking at the contributions to the partition function of the central configurations of the tree in Fig. 3, we may write down the average number of monomers, polymers, and bonds per site x_m, x_p, and x_b, respectively, in the central region. For the central site of the M-generation Cayley tree we get

$$
\begin{aligned}
x_{m,M} &= \left\langle \sum_i v_i \right\rangle \Big/ N = 1 - [\omega_{00}\, g_M(u_0) + \omega_{01}\, g_M(u_1)]^q\, Y_M^{-1} \\
x_{p,M} &= \langle N_p \rangle / N = \omega_1 \{ K_1 [\omega_{01}\, g_M(u_0) + \omega_{11}\, g_M(u_1)]^q \\
&\quad + \tfrac{1}{2} q (2K_1 K_p')^{1/2}\, \omega_{11}\, g_M(b) [\omega_{01} g_M(u_0) + \omega_{11}\, g_M(u_1)]^{q-1} \}\, Y_M^{-1} \\
x_{b,M} &= \langle N_b \rangle / N = \omega_1 \{ \tfrac{1}{2} q (2K_1 K_p')^{1/2}\, \omega_{11}\, g_M(b) \\
&\quad \times [\omega_{01}\, g_M(u_0) + \omega_{11}\, g_M(u_1)]^{q-1} + \tfrac{1}{2} q(q-1) \omega_{11}^2 K_p'\, g_M^2(b) \\
&\quad \times [\omega_{01}\, g_M(u_0) + \omega_{11}\, g_M(u_1)]^{q-2} \}\, Y_M^{-1}
\end{aligned}
\tag{3.8}
$$

In the calculation for x_p, we count one polymer if an unbonded active monomer is on the central site and only one-half polymer if a chain consisting of more than one monomer ends there. This ensures that if a similar average is performed at each site and these are summed, each polymer is counted exactly once. In terms of the variables R and S, in the thermodynamic limit these expressions may be rewritten

$$x_m = 1 - \frac{[S+1]^q}{D}$$

$$x_p = \frac{\omega_{\bar{A}}\{K_1[S+\omega_{\bar{K}}]^q + \tfrac{1}{2}q(2K_1)^{1/2}\,\omega_{\bar{K}} R[S+\omega_{\bar{K}}]^{q-1}\}}{D} \tag{3.9}$$

$$x_b = \frac{\omega_{\bar{A}}\{\tfrac{1}{2}q(2K_1)^{1/2}\omega_{\bar{K}} R[S+\omega_{\bar{K}}]^{q-1} + \tfrac{1}{2}q(q-1)\,\omega_{\bar{K}}^2 R^2[S+\omega_{\bar{K}}]^{q-2}\}}{D}$$

where

$$D = [S+1]^q + \omega_{\bar{A}}\{(1+K_1)[S+\omega_{\bar{K}}]^q + q(2K_1)^{1/2}\,\omega_{\bar{K}} R[S+\omega_{\bar{K}}]^{q-1} + \tfrac{1}{2}q(q-1)\,\omega_{\bar{K}}^2 R^2[S+\omega_{\bar{K}}]^{q-2}\}$$

and where R and S are fixed-point values of the recursion relation (3.5) ($R_{M+1} = R_M = R$ and $S_{M+1} = S_M = S$). The fraction of core sites incorporated into polymers will be

$$\phi_\mu = x_b + x_p \tag{3.10}$$

It is straightforward to show that the same averages are obtained for nearest neighbor sites to the central site in the thermodynamic limit and, as happens in the case of the Ising model,[23] we believe that these results are valid for sites within any finite range of the central site if the thermodynamic limit is taken first.

We have, therefore, reduced the solution of the model on the Bethe lattice to a two-dimensional mapping problem. For given values of the parameters K_1, K_p', $\omega_{\bar{K}}$, and $\omega_{\bar{A}}$, the variables R_M and S_M will attain a fixed point (R, S) in the thermodynamic limit $M \to \infty$ and the relevant properties will be given by the values of expressions (3.9) at the fixed point. In Sections 4 and 5 phase diagrams are obtained using this procedure, but first it is instructive to look at some limits of our Bethe-lattice solution.

3.1. Pure Monomer Limit

The absence of any solvent may be accomplished by taking the limit $\omega_1 \to \infty$, or $\omega_{\bar{A}} \to \infty$. The recursion relations (3.5) then reduce to

$$R_{M+1} = \frac{(2K_1)^{1/2}\,K_p' + (q-1)\,K_p' R_M}{(1+K_1) + (q-1)(2K_1)^{1/2} R_M + \tfrac{1}{2}(q-1)(q-2)\,R_M^2}$$

$$S_{M+1} = 0 \tag{3.11}$$

The thermodynamic properties in (3.9) will be given by

$$\begin{aligned} x_m &= 1 \\ x_p &= \frac{K_1 + \frac{1}{2}q(2K_1)^{1/2}R}{1 + K_1 + q(2K_1)^{1/2}R + \frac{1}{2}q(q-1)R^2} \\ x_b &= \frac{\frac{1}{2}q(2K_1)^{1/2}R + \frac{1}{2}q(q-1)R^2}{1 + K_1 + q(2K_1)^{1/2}R + \frac{1}{2}q(q-1)R^2} \end{aligned} \tag{3.12}$$

The behavior of the model in this limit is considered in Section 4.

3.2. Lattice Gas Limit

The occurrence of polymerization may be suppressed by letting K_1 and K_p vanish. The recursion relations (3.5) turn into

$$R_{M+1} = 0, \qquad S_{M+1} = \frac{[S_M + 1]^{q-1}}{\omega_{\bar{A}}[S_M + \omega_{\bar{K}}]^{q-1}} \tag{3.13}$$

and we get

$$\begin{aligned} x_m &= 1 - \frac{[S+1]^q}{[S+1]^q + \omega_{\bar{A}}[S + \omega_{\bar{K}}]^q} \\ x_p &= x_b = 0 \end{aligned} \tag{3.14}$$

As expected, the Bethe lattice results for an Ising lattice gas are recovered in this limit.[15]

3.3. One-Dimensional Limit

When $q = 2$, the Bethe lattice solution corresponds to the exact solution of the one-dimensional model,[18] Some results for this limit may be found in Appendix A.

3.4. Mean-Field Limit ($q \to \infty$)

By properly taking the limit of an infinite coordination number, we recover the already known mean-field results for the equilibrium polymerization in a solvent.[1,2a,2b] It is helpful to define the quantities

$$Q_M \equiv qR_M, \qquad K_p \equiv qK'_p, \qquad \tilde{\kappa} \equiv q\tilde{K} \tag{3.15}$$

Now, the recursion relations (3.5) may be rewritten in terms of these parameters. In the limit $q \to \infty$, with K_p and $\tilde{K}$ constant, they become

$$\begin{aligned} Q_{M+1} &= \frac{(2K_1)^{1/2}K_p + K_p Q_M(1/[S_M+1])}{1+K_1+(2K_1)^{1/2}Q_M(1/[S_M+1]) + \frac{1}{2}Q_M^2/[S_M+1]^2} \\ S_{M+1} &= \frac{\exp[-\tilde{\kappa}/(1+S_M)]}{\omega_{\bar{A}}\{1+K_1+(2K_1)^{1/2}Q_M/[S_M+1] + \frac{1}{2}Q_M^2/[S_M+1]^2\}} \end{aligned} \tag{3.16}$$

In the thermodynamic limit, a fixed point (Q, S) will be reached, given by

$$\begin{aligned} Q &= \frac{K_p[(2K_1)^{1/2} + Q/(1+S)]}{1+\frac{1}{2}[(2K_1)^{1/2}+Q/(1+S)]^2} \\ S &= \frac{1}{\omega_{\bar{A}}\exp[\tilde{\kappa}/(1+S)]\{1+\frac{1}{2}[(2K_1)^{1/2}+Q/(1+S)]^2\}} \end{aligned} \tag{3.17}$$

The densities (3.9) in the $q \to \infty$ limit will be

$$\begin{aligned} x_m &= 1 - \frac{\exp[-\tilde{\kappa}/(1+S)]}{\exp[-\tilde{\kappa}/(1+S)] + \omega_{\bar{A}}\{1+K_1+(2K_1)^{1/2}Q/(1+S) + \frac{1}{2}Q^2/[1+S]^2\}} \\ x_p &= \frac{\omega_{\bar{A}}\{K_1 + \frac{1}{2}(2K_1)^{1/2}Q/(1+S)\}}{\exp[-\tilde{\kappa}/(1+S)] + \omega_{\bar{A}}\{1+K_1+\frac{1}{2}(2K_1)^{1/2}Q/(1+S) + \frac{1}{2}[Q/(1+S)]^2\}} \\ x_b &= \frac{\omega_{\bar{A}}\{\frac{1}{2}(2K_1)^{1/2}Q/(1+S) + \frac{1}{2}[Q/(1+S)]^2\}}{\exp[-\tilde{\kappa}/(1+S)] + \omega_{\bar{A}}\{1+K_1+\frac{1}{2}(2K_1)^{1/2}Q/(1+S) + \frac{1}{2}[Q/(1+S)]^2\}} \end{aligned} \tag{3.18}$$

Now we notice that

$$x_m = 1/(1+S) \tag{3.19}$$

so that S may be eliminated, resulting in

$$\begin{aligned} Q &= \frac{K_p[(2K_1)^{1/2} + Qx_m]}{1+\frac{1}{2}[(2K_1)^{1/2}+Qx_m]^2} \\ (1-x_m)^{-1} &= 1 + \omega_{\bar{A}}[\exp(\tilde{\kappa}x_m)]\{1+\tfrac{1}{2}[(2K_1)^{1/2}+Qx_m]^2\} \\ x_p + x_b &= \frac{\omega_{\bar{A}}[\exp(\tilde{\kappa}x_m)]\,\frac{1}{2}[(2K_1)^{1/2}+Q\phi_s]^2}{1+\omega_{\bar{A}}[\exp(\tilde{\kappa}x_m)]\{1+\frac{1}{2}[(2K_1)^{1/2}+Q\phi_s]^2\}} \end{aligned} \tag{3.20}$$

To compare these results with the ones obtained by Wheeler and Pfeuty,[2a,2b] it is necessary to rewrite them using dilute $n \to 0$ vector model parameters, where now q is the (finite) coordination number of the trans-

lationally invariant lattice on which the mean field approximation is being made:

$$\tilde{\kappa} = qK, \qquad K_p = q\tilde{J}, \qquad K_1 = h^2/2 \tag{3.21}$$

$$x_p + x_b = \tfrac{1}{2}m(q\tilde{J}m + h), \qquad x_m = x_s \tag{3.21}$$

and, eliminating Q in the expression (3.20), we have

$$\begin{aligned} (1-x_s)^{-1} &= 1 + \omega_{\tilde{A}}[\exp(qKx_s)][1 + \tfrac{1}{2}(h + q\tilde{J}m)^2] \\ m &= \frac{\omega_{\tilde{A}}[\exp(qKx_s)](h + q\tilde{J}m)}{1 + \omega_{\tilde{A}}[\exp(qKx_s)][1 + \tfrac{1}{2}(h + q\tilde{J}m)^2]} \end{aligned} \tag{3.22}$$

These are the mean-field results for the dilute $n \to 0$ vector model obtained by Wheeler and Pfeuty [expressions (5.14) and (5.15) of Ref. 2b].

4. THE LIMITING CASE OF EQUILIBRIUM POLYMERIZATION IN THE ABSENCE OF A SOLVENT

In this section we will discuss the particular case where no solvent is present, which was already considered by Gujrati[22] when $q = 3$. As we saw in Section 3, in the limit $\omega_{\tilde{A}} \to \infty$ the solution of the model reduces to a one-dimensional mapping (3.11). In the case of liquid sulfur, the appropriate value for the statistical weight K_1 is very small[1a,1b] ($K_1 \sim 10^{-12}$). Thus, we will concentrate our attention on the results with $K_1 \to 0$. In this limit, the fixed points of Eq. (3.11) will be the solution of

$$\tfrac{1}{2}(q-1)(q-2)R^3 + [1 - (q-1)K_p']R = 0 \tag{4.1}$$

which are

$$R = 0, \qquad \pm\left\{\frac{2[(q-1)K_p' - 1]}{(q-1)(q-2)}\right\}^{1/2} \tag{4.2}$$

corresponding, respectively, to the unpolymerized and polymerized phases. The critical temperature will be given by

$$K_{p,c}' = 1/(q-1) \tag{4.3}$$

The fraction of monomers incorporated into polymers is given by

$$\phi_\mu = x_p + x_b = \frac{(q-1)K_p' - 1}{(q-1)K_p' - 2/q} \tag{4.4}$$

We may introduce a reduced temperature τ through

$$K_p' = \frac{1}{q-1} \exp\left[3.70\left(1 - \frac{1}{\tau}\right)\right] \tag{4.5}$$

a parametrization appropriate for liquid sulfur and sulfur solutions.[2a,2b] Expression (4.4) may then be rewritten as

$$\phi_\mu = \frac{\exp[3.70(1 - 1/\tau)] - 1}{\exp[3.70(1 - 1/\tau)] - 2/q} \tag{4.6}$$

In Fig. 4 we present some curves of ϕ_μ versus τ. The behavior of ϕ_μ becomes steeper as the critical temperature is approached for decreasing q. This is in accord with the expectation that with increased range of correlations the curve will approximate that of translationally invariant lattices where the limiting slope is infinite and is described by the nonclassical exponent α of the $n \to 0$ vector model.[1a,1b] Of course, asymptotically, ϕ_μ is

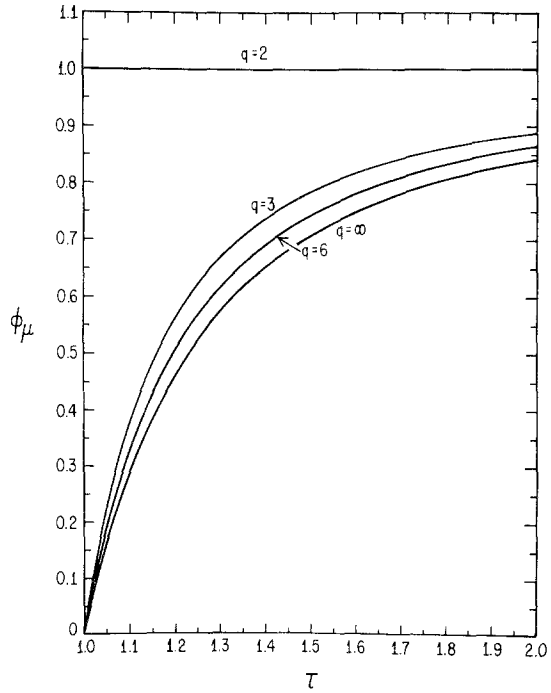

Fig. 4. Curves ϕ_μ versus τ for pure monomer. Results for the mean-field limit ($q \to \infty$), $q = 6$, $q = 3$, and $q = 2$ are shown.

always linear in τ for $\tau \to 1^+$, since the Bethe-lattice calculation produces classical critical exponents. At $q=2$, the step-function behavior from $\phi_\mu = 0$ to $\phi_\mu = 1$ of the 1D model[18] is recovered.

For $q=3$, our results may be compared to the ones obtained by Gujrati.[22] We verified that they agree, if the proper correspondence is made between the formulations of the equilibrium polymerization problem by Wheeler and Pfeuty[1b] and by Gujrati.[24] In Gujrati's formulation, only polymers with at least one bond are considered. The relations between Gujrati's[22] variables κ and η and the ones in our formulation are

$$\kappa = \frac{K_p'}{1+K_1}, \qquad \eta = \left(\frac{2K_1}{1+K_1}\right)^{1/2} \tag{4.7}$$

and the variable x used by Gujrati in the recursion relation is related to our R as follows:

$$x = R/(K_p')^{1/2} \tag{4.8}$$

The relations between the densities in our formulation (x_b, x_p) and those from Gujrati's (ϕ_l, ϕ_p) are

$$x_b = \phi_l, \qquad x_p = \phi_p + \frac{K_1}{1+K_1}(1-\phi_l-\phi_p) \tag{4.9}$$

The second term in (4.9) has a clear physical meaning, corresponding to the density of one-site (zero-bond) polymers. {A misprint in the intermediate expression for ϕ_e [expression (10) of Ref. 22] should be pointed out. In the numerator $2Z_0(1)\,Z_1^2(0)\omega_2$ should be replaced by $2Z_0(1)\,Z_1(1)\,Z_1(0)\omega_2$.}

5. PHASE DIAGRAMS

It is convenient to classify the fixed points (for $K_1 \to 0$) of the recursion relations (3.5) into two categories:

5.1. Unpolymerized Fixed Points ($R=0$)

We notice that $(R=0, S)$ is always a fixed point of Eqs. (3.5), S being given by

$$S = [S+1]^{q-1}/\omega_{\bar{A}}[S+\omega_{\bar{K}}]^{q-1} \tag{5.1}$$

This corresponds to the Ising lattice gas problem on the Bethe lattice.

5.2. Polymerized Fixed Points ($R \neq 0$)

In this case Eq. (3.5) will have a fixed point given by

$$S = \frac{[S+1]^{q-1}}{\omega_{\tilde{A}}(q-1)\,\omega_{\tilde{K}} K_p'[S+\omega_{\tilde{K}}]^{q-2}} \tag{5.2}$$

and

$$R^2 = \frac{2K_p'[S+\omega_{\tilde{K}}]}{(q-2)\omega_{\tilde{K}}} - \frac{2[S+\omega_{\tilde{K}}]^2}{(q-1)(q-2)\omega_{\tilde{K}}^2} \tag{5.3}$$

For the pure sulfur case, $S=0$, and therefore the critical polymerization condition on the Bethe lattice is given by Eq. (4.3). Also, the upper critical solution point, where two coexisting unpolymerized phases become identical, is fixed by the conditions

$$(\partial\omega_{\tilde{A}}/\partial S)_{\omega_{\tilde{K}}} = 0, \qquad (\partial^2\omega_{\tilde{A}}/\partial S^2)_{\omega_{\tilde{K}}} = 0 \tag{5.4}$$

the variable $\omega_{\tilde{A}}$ being given as a function of S by (5.1). Actually, the density conjugate to the field $\tilde{A}$ is x_m, but since x_m is a monotonically decreasing function of S, we may use the conditions (5.4) for locating the upper critical solution point. The result is

$$\omega_{\tilde{K}} = \omega_{\tilde{K},1} \equiv [q/(q-2)]^2 \tag{5.5}$$

If we introduce the parameter α by the ratio

$$\alpha = T_p^*/T_1 \tag{5.6}$$

between the critical polymerization temperature T_p^* of pure sulfur and the upper critical temperature T_1, we can establish a parametrization convenient for sulfur solutions, similar to the one used by Wheeler and Pfeuty,[2a,2b] given by Eq. (4.5) and

$$\omega_{\tilde{K}} = \exp\left[\frac{2}{\alpha\tau}\ln\left(\frac{q}{q-2}\right)\right] \tag{5.7}$$

With this parametrization, the critical polymerization temperature for pure sulfur will occur at $\tau = 1$, whereas the upper critical temperature corresponds to $\tau = 1/\alpha$.

The results for the phase diagrams that will be presented were all obtained for $\alpha = 1$. One of the ways to obtain the phase diagrams is to study isotherms in the x_m, $\tilde{A}$ plane. It is more convenient to use the "activity fraction"

$$\zeta \equiv \frac{\omega_{\tilde{A}}}{1+\omega_{\tilde{A}}} = \frac{\exp(\mu_1/kT)(\omega_{01}/\omega_{00})^q}{\exp(\mu_0/kT)+\exp(\mu_1/kT)(\omega_{01}/\omega_{00})^q} \tag{5.8}$$

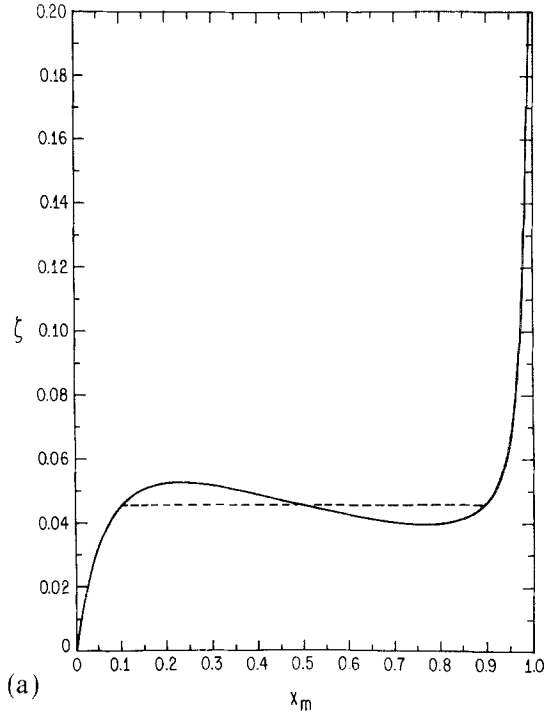

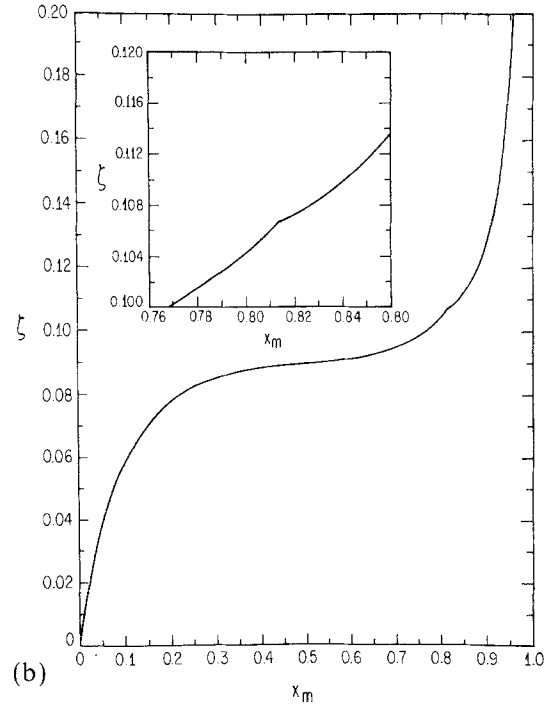

Fig. 5. Isotherms in the xm, ζ plane for $q = 6$. (a) $\tau = 0.8$, (b) $\tau = 1.05$, and (c) $\tau = 1.2$.

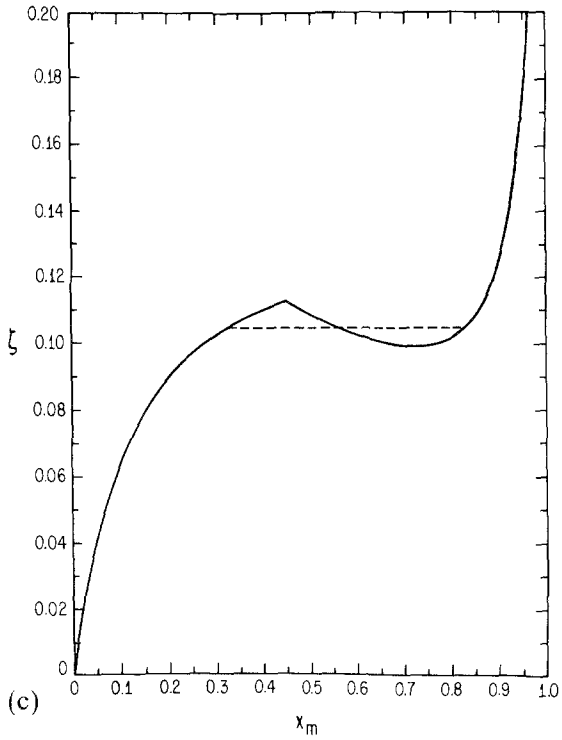

Fig. 3 (*continued*)

in place of $\tilde{A}$. In Fig. 5, three of these isotherms are shown, for temperatures $\tau = 0.8$, 1.05, and 1.2. At $\tau = 0.8$, a first-order transition between two unpolymerized phases is apparent. The value of ζ at the transition may be obtained using the equal-area rule, by performing the integrations $\int \tilde{A}\, dx_m$, or, more easily, taking advantage of the isomorphism of the model with the Ising model, where the transition is known to happen when the magnetic field vanishes. This leads to the following expression for the first-order boundary:

$$\omega_{\tilde{A}} = [\omega_{\tilde{K}}]^{-q/2} \tag{5.9}$$

the critical point being located at, from (5.5) and (5.7),

$$\tau_1 = 1, \qquad \zeta_1 = \frac{1}{1 + [(q-2)/q]^q}, \qquad x_{m,1} = \frac{1}{2} \tag{5.10}$$

Also, it is easy to obtain the expressions for the spinodal lines associated to this transition. Using the condition

$$(\partial \omega_{\tilde{A}} / \partial S)_{\omega_{\tilde{K}}} = 0$$

we get

$$S_{\pm} = \frac{(q-2)\omega_{\bar{K}} - q \pm \{[(q-2)\omega_{\bar{K}} - q]^2 - 4\omega_{\bar{K}}\}^{1/2}}{2} \tag{5.11}$$

and the corresponding values of $\omega_{\bar{A}}$ and ζ may be calculated using (5.1) and (5.8). We will show later that the spinodal lines correspond to the stability limit of the fixed points associated with the two coexisting phases.

At $\tau = 1.05$, the isotherm has two branches. For high values of ζ the branch corresponding to the polymerized fixed point is stable, whereas at the low ζ the unpolymerized fixed point will be attained. Both branches meet at a point described by

$$S = \omega_{\bar{K}}[(q-1)K_p' - 1] \tag{5.12}$$

where the second-order polymerization transition occurs. This point is shown amplified in the insert to Fig. 5b.

At higher temperatures ($\tau = 1.2$, Fig. 5c), it is apparent that the polymerization transition has changed to first order, the spinodal line given by the condition

$$S = \frac{\omega_{\bar{K}}}{\omega_{\bar{K}}(q-2) - (q-1)} \tag{5.13}$$

The curves given by expressions (5.12) and (5.13) will be shown below to correspond to the stability limits of the unpolymerized and polymerized phases, respectively.

Again an equal-area calculation is performed to locate the first-order transition. In the mean-field limit, we show in Appendix B that the integration can be done analytically so that the expression for the free energy is obtained from the fixed-point equations (3.17). For the Bethe-lattice solution, we performed the integrations numerically.

It is interesting that no difficulty arises in the equal-area construction even though the isotherm consists of two intersecting branches with different functional form (see Fig. 5c). In the case of fluid–solid phase equilibrium there is often a problem of correctly assigning the difference in the zero of the free energy of the two phases. That problem does not arise here because, as in the case of equilibrium between fluid phases, it is possible to analytically continue from one phase to the other around the (tri) critical point, avoiding the first-order phase transition altogether. In the present case this involves continuing through the polymerization transition, across which x_m, $\bar{A}$, and the free energy are all continuous.

It should be stressed that the validity of the equal-area construction depends upon the existence of an underlying thermodynamic potential

from which the various densities can be obtained. This is, of course, certainly true if the densities corresponding to the exact results for the full Cayley tree are considered, but is by no means so simple to guarantee for the averages calculated on interior sites. For the unpolymerized branch of the solution of the equilibrium polymerization problem on the Bethe lattice, the existence of an underlying potential is assured, since the model is isomorphic to the Ising model in this case, whose free energy on the Bethe lattice was obtained by Thompson.[19] We did not verify this analytically for the polymerized branch for $2 < q < \infty$, due to the algebraic complexity of the calculation involved. Nevertheless, we are confident that there exists an underlying poential for this case as well, since we verified numerically, at a significant number of points in the field space, that the densities obey the required Maxwell relations for $K_1 = 0$:

$$\begin{aligned} \partial x_b/\partial \tilde{\Delta} &= \partial x_m/\partial(\ln K_p') \\ \partial x_b/\partial \tilde{K} &= \partial e_I/\partial(\ln K_p') \\ \partial x_m/\partial \tilde{K} &= \partial e_I/\partial \tilde{\Delta} \end{aligned} \tag{5.14}$$

where the density e_I is defined by

$$e_I = \frac{1}{N}\left\langle \sum_{\langle ij \rangle} \nu_i \nu_j \right\rangle \tag{5.15}$$

The tricritical point, where the polymerization transition changes from second to first order, may be defined as the point where the curves given by Eqs. (5.12) and (5.13) meet. Thus, the tricritical condition is

$$(q-1)K_p' = \frac{1}{\omega_{\tilde{K}}(q-2)-(q-1)} + 1 \tag{5.16}$$

In Fig. 6, the ζ versus τ phase diagrams are displayed for $q = 3$, 6, and 500. The results for $q = 500$ are indistinguishable from the man-field results in the scale of the diagrams. The corresponding x_m versus τ phase diagrams may be seen in Fig. 7.

Although our Bethe-lattice results are classical with regard to the critical region, comparison of the phase diagrams for finite $q > 2$ with the one for $q \to \infty$ shows that the differences are in accord with expectations. In particular, the broadening of the coexistence curve with τ larger than the tricritical value should be noted, since it is a prediction of the scaling hypothesis with logarithmic corrections in the vicinity of the tricritical point.[2b] Of course, the unpolymerized branch of the coexistence curve still meets the critical line tangentially at the tricritical point, and both branches

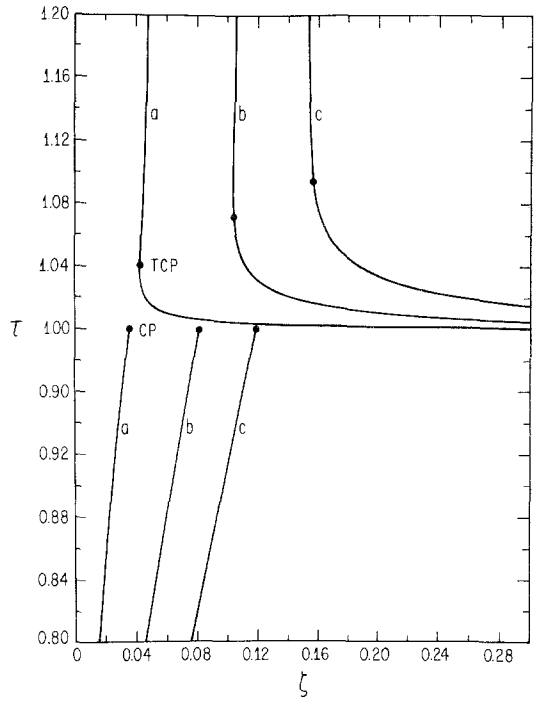

Fig. 6. Phase diagrams in the ζ, τ space for (a) $q=3$, (b) $q=6$, and (c) $q=500$.

of the coexistence curve meet, forming an angle smaller than π, as is expected for any mean-field-like theory. Nevertheless, the angle between the two branches of the coexistence curve increases with decreasing values of q. This is also in closer accord with the phase diagrams for sulfur with toluene, *o*-xylene, and triphenylmethane, and *cis*-decalin,[7,8,25] which show a rounded coexistence curve at high temperatures. Incidentally, the same effect is observed in a Flory–Huggins theory that allows for polymeric rings,[26] thus providing an alternative explanation for the experimentally observed phase diagrams.

Finally, it is worthwhile to perform a linear stability analysis of the recursion relations in the vicinity of the fixed points. Let us define the deviations from the fixed point,

$$\Delta R_M = R_M - R, \qquad \Delta S_M = S_M - S \tag{5.17}$$

and the linearized recursion relations are

$$\Delta R_{M+1} = f_{11}\,\Delta R_M + f_{12}\,\Delta S_M, \qquad \Delta R_{M+1} = f_{21}\,\Delta R_M + f_{22}\,\Delta S_M \tag{5.18}$$

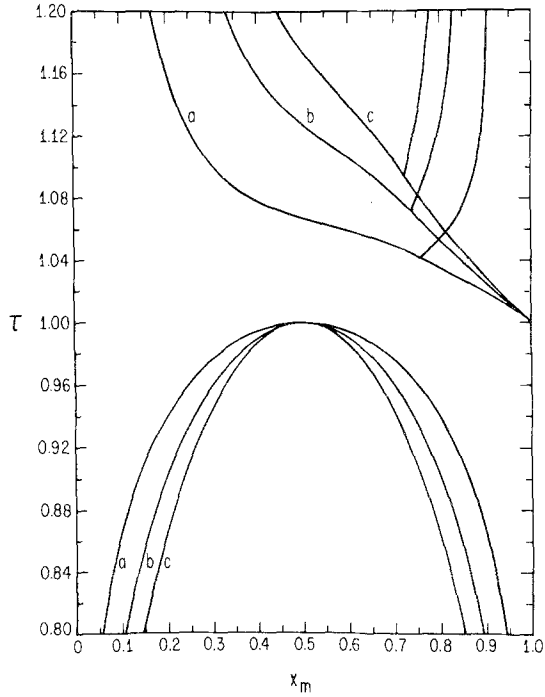

Fig. 7. Phase diagrams in the x_m, τ space for (a) $q=3$, (b) $q=6$, and (c) $q=500$. Here (c) corresponds, in the scale of the figure, to the mean-field results depicted in Fig. 3a of Ref. 2b.

with

$$f_{11}=\left.\frac{\partial R_{M+1}}{dR_M}\right|_{R,S}, \qquad f_{12}=\left.\frac{\partial R_{M+1}}{\partial S_M}\right|_{R,S}$$
$$f_{21}=\left.\frac{\partial S_{M+1}}{\partial R_M}\right|_{R,S}, \qquad f_{22}=\left.\frac{\partial S_{M+1}}{\partial S_M}\right|_{R,S} \tag{5.19}$$

The derivatives may be evaluated from the recursion relations (3.5). For $K_1=0$, we get the following result for the unpolymerized fixed points (5.1):

$$f_{11}=(q-1)\,\omega_{\bar{K}}K_p'/(S+\omega_{\bar{K}})$$
$$f_{12}=f_{21}=0 \tag{5.20}$$
$$f_{22}=[(q-1)S/(S+1)](\omega_{\bar{K}}-1)/(S+\omega_{\bar{K}})$$

At the polymerized fixed points (5.2)–(5.3), the derivatives are given by

$$
\begin{aligned}
f_{11} &= \frac{2(S+\omega_{\bar{K}})}{(q-1)\,\omega_{\bar{K}} K_p'} - 1 \\
f_{12} &= \frac{R}{S+\omega_{\bar{K}}}\left[1 - \frac{2(S+\omega_{\bar{K}})}{(q-1)\,\omega_{\bar{K}} K_p'}\right] \\
f_{21} &= -RS\frac{(q-2)\,\omega_{\bar{K}}}{K_p(S+\omega_{\bar{K}})} \\
f_{22} &= \frac{(q-1)S}{S+1} - \frac{S}{\omega_{\bar{K}} K_p'(q-1)}\left[\frac{(q-1)(q-3)\,\omega_{\bar{K}} K_p}{S+\omega_{\bar{K}}} + 2\right]
\end{aligned}
\tag{5.21}
$$

The stability limit of a fixed point is reached when the largest eigenvalue of the matrix $\mathbf{f}$ becomes equal to unity. For the unpolymerized fixed points, the matrix $\mathbf{f}$ is diagonal and the eigenvalues are $\lambda_1 = f_{11}$ and $\lambda_2 = f_{22}$. There are two possible stability limit conditions: $\lambda_1 = 1$ and $\lambda_2 = 1$. Now it is possible to verify that $\lambda_2 < 1$ when $\lambda_1 = 1$ and that $\lambda_1 < 1$ when $\lambda_2 = 1$. Thus, $\lambda_1 = 1$ gives us the spinodal lines (5.11), whereas $\lambda_2 = 1$ is the condition (5.12), corresponding to the second-order boundary at temperatures between T_p^* and the tricritical temperature and to the stability limit of the unpolymerized phase above the tricritical temperature.

The largest eigenvalue of the matrix of the linearized recursion relations for the polymerized phase (5.21) is equal to unity if the following condition is fulfilled.

$$
\left[\frac{S+\omega_{\bar{K}}}{(q-1)\,\omega_{\bar{K}} K_p'} - 1\right]\left[\frac{(q-1)S}{S+1} - \frac{(q-2)S}{S\omega_{\bar{K}}} - 1\right] = 0 \tag{5.22}
$$

At temperatures between T_p^* and the tricritical temperatures, condition (5.12) describes the stability limit of the polymerized fixed points, whereas at temperatures above the tricritical temperature the vanishing of the second factor in (5.22) occurs first and the stability limit will be given by Eq. (5.13).

6. SOLUTION OF THE DILUTE $n \to 0$ VECTOR MODEL ON THE CAYLEY TREE

A correspondence exists[2] between the model for equilibrium polymerization in a solvent and the dilute n-vector model in the limit $n \to 0$, with the Hamiltonian

$$
\mathcal{H} = -K\sum_{\langle ij\rangle} v_i v_j - \Delta\sum_i v_i - J\sum_{\langle ij\rangle} v_i v_j \mathbf{S}_i \cdot \mathbf{S}_j - m_0 H\sum_i v_i S_i^{(1)} \tag{6.1}
$$

where the sum $\sum_{\langle ij\rangle}$ is over nearest neighbor pairs, the v_i are Ising lattice gas variables ($v_i = 0, 1$), and $\mathbf{S}$ is a classical spin of n components with norm $\sqrt{n}$ and whose first component points in the direction of the magnetic field H. In the formal limit $n \to 0$, the partition function of this model can be written as[2a,2b]

$$Z = \sum_{\{v_i\}} \exp\left(\tilde{K} \sum_{\langle ij\rangle} v_i v_j + \tilde{\Delta} \sum_i v_i\right) \sum_{N_b} \sum_{N_p} \sum_{N_1} (\tilde{J})^{N_b} (h^2)^{N_b} (\tfrac{1}{2})^{N_1} \times \Gamma(N_p, N_b, N_1, N, \{v_i\}) \tag{6.2}$$

where

$$\tilde{J} = J/k\tilde{T}, \qquad \tilde{K} = K/k\tilde{T}, \qquad \tilde{\Delta} = \Delta/k\tilde{T}, \qquad h = m_0 H/k\tilde{T} \tag{6.3}$$

$\tilde{T}$ being the temperature of the $n \to 0$ vector model. Comparison of (6.2) and (2.2) shows that the equivalence between the models may be established as

$$Y = \exp(-\tfrac{1}{2} q N E_{00}/kT)\, Z(\tilde{K}, \tilde{J}, \tilde{h}, \tilde{\Delta}) \tag{6.4}$$

if

$$\tilde{J} = K_p', \qquad \tfrac{1}{2} h^2 = K_1$$
$$\tilde{\Delta} = [\mu_1 - \mu_0 - q(E_{01} - E_{00})]/kT, \qquad \tilde{K} = (2E_{01} - E_{00} - E_{11})/kT \tag{6.5}$$

Now we will show how it is possible to solve the dilute $n \to 0$ vector model (6.1) on the Bethe lattice, recovering the results of the direct calculations. Thus, we define the following partial partition functions for an M-generation subtree with site i at the root, where the trace is over the values of all spins in the subtree, with the exception of the spin $\mathbf{S}_i$ located at the root

$$g_M(1, \mathbf{S}_i) = \operatorname*{Tr}_{\substack{\mathbf{S} \neq \mathbf{S}_i \\ v_i = 1}} \exp(-H/k\tilde{T})$$
$$g_M(0) = \operatorname*{Tr}_{(v_i = 0)} \exp(-H/k\tilde{T}) \tag{6.6}$$

the Hamiltonian being given by (6.1). We may then obtain recursion relations for the g's by constructing an $(M+1)$-generation subtree from $q-1$ of the M-generation subtrees,

$$g_{M+1}(1, \mathbf{S}) = \operatorname*{Tr}_{\mathbf{S}'} \{\exp[\tilde{K} + \tilde{\Delta} + \tilde{J}\mathbf{S} \cdot \mathbf{S}' + hS'^{(1)}][g_M(1, \mathbf{S}')]^{q-1}\} + [g_M(0)]^{q-1}$$
$$g_{M+1}(0) = \operatorname*{Tr}_{\mathbf{S}'} \{\exp[\tilde{\Delta} + hS'^{(1)}][g_M(1, S')]^{q-1}\} + [g_M(0)]^{q-1} \tag{6.7}$$

where $\tilde{K}$, $\tilde{J}$, $\tilde{\Delta}$, and defined in (6.3). Next, we make the following ansatz for the functional form of the g_M, which can be shown to be right by induction later:

$$g_M(1, \mathbf{S}) = a_M + b_M S^{(1)}, \qquad g_M(0) = c_M \tag{6.8}$$

It is then possible to calculate the traces in (6.7) explicitly, in the $n \to 0$ limit, by expanding the function involving $\mathbf{S}'$, and remembering that in the limit $n \to 0$ we should define the trace operation to be the angular average over the spins and that,[1a,1b] when $b \to 0$,

$$\langle (S_i^{(\alpha)})^k \rangle_A = \delta_{k,0} + \delta_{k,2} \tag{6.9}$$

the δ's being Kronecker functions. Thus, in the $n \to 0$ limit the trace operation is simplified considerably, and from (6.2) and (6.3) it follows that

$$\begin{aligned}
a_{M+1} &= \omega_{\tilde{K}} \omega_{\tilde{\Delta}} [(1 + \tfrac{1}{2}h^2)\, a_M^{q-1} + (q-1)\, h b_M a_M^{q-1} \\
&\quad + \tfrac{1}{2}(q-1)(q-2)\, a_M^{q-3} b_M^2] + c_M^{q-1} \\
b_{M+1} &= \omega_{\tilde{K}} \omega_{\tilde{\Delta}} [\tilde{J} h a_M^{q-1} + (q-1)\, \tilde{J} a_M^{q-2} b_M] \\
c_{M+1} &= \omega_{\tilde{\Delta}} [(1 + \tfrac{1}{2}h^2)\, a_M^{q-1} + (q-1)\, h b_M a_M^{q-2} \\
&\quad + \tfrac{1}{2}(q-1)(q-2)\, a_M^{q-3} b_M^2] + c_M^{q-1}
\end{aligned} \tag{6.10}$$

where $\omega_{\tilde{\Delta}}$ and $\omega_{\tilde{K}}$ are $\exp \tilde{\Delta}$ and $\exp \tilde{K}$, respectively.

The partition function may be obtained by attaching q M-generation subtrees together at a central site. The result is

$$Z_M = \omega_{\tilde{\Delta}} [a_M^q (1 + \tfrac{1}{2}h^2) + q h a_M^{q-1} b_M + \tfrac{1}{2} q(q-1)\, a_M^{q-2} b_M^2] + c_M^q \tag{6.11}$$

The central site magnetization, energy per spin pair, and occupancy expectation number are found to be

$$m_M = \omega_{\tilde{\Delta}} (h a_M^q + q a_M^{q-1} b_M) Z_M^{-1} \tag{6.12}$$

$$\hat{e}_M = \omega_{\tilde{\Delta}} \tilde{J}^{-1} [h b_M a_M^{q-1} + (q-1) b_M^2 a_M^{q-2}] Z_M^{-1} \tag{6.13}$$

and

$$\phi_{s,M} = \omega_{\tilde{\Delta}} [(1 + \tfrac{1}{2}h^2) a_M^q + q h a_M^{q-1} b_M + \tfrac{1}{2} q(q-1)\, a_M^{q-2} b_M^2] Z_M^{-1} \tag{6.14}$$

The comparison with the results of the direct calculation is straightforward if we define

$$R_M \equiv \frac{\omega_{\tilde{K}} - 1}{\omega_{\tilde{K}}} \frac{b_M}{a_M - c_M} \tag{6.15}$$

$$S_M \equiv \frac{c_M \omega_{\tilde{K}} - a_M}{a_M - c_M} \tag{6.16}$$

From the recursion relations (6.10) for the a's, b's, and c's the results (3.5) from the direct solution follow, using the transcriptions (6.5). Also, (6.12)–(6.14) may be written in terms of the R_M and S_M, giving

$$m_M = \omega_{\tilde{A}}\left[h + qR_M\frac{\omega_{\tilde{K}}}{S_M+\omega_{\tilde{K}}}\right] \times\left\{\omega_{\tilde{A}}\left[1+\frac{h^2}{2}+qhR_M\frac{\omega_{\tilde{K}}}{S_M+\omega_{\tilde{K}}} + \frac{q(q-1)}{2}R_M^2\left(\frac{\omega_{\tilde{K}}}{S_M+\omega_{\tilde{K}}}\right)^2\right]+\left[\frac{S_M+1}{S_M+\omega_{\tilde{K}}}\right]^q\right\}^{-1} \tag{6.17}$$

$$\hat{e}_M = \omega_{\tilde{A}}\left[hR_M\frac{\omega_{\tilde{K}}}{S_M+\omega_{\tilde{K}}}+(q-1)R_M^2\left(\frac{\omega_{\tilde{K}}}{S_M+\omega_{\tilde{K}}}\right)^2\right] \times\left(\tilde{J}\left\{\omega_{\tilde{A}}\left[1+\frac{h^2}{2}+qhR_M\frac{\omega_{\tilde{K}}}{S_M\omega_{\tilde{K}}} + q\frac{q-1}{2}R_M^2\left(\frac{\omega_{\tilde{K}}}{S_M+\omega_{\tilde{K}}}\right)^2\right]+\left[\frac{S_M+1}{S_M+\omega_{\tilde{K}}}\right]^q\right\}\right)^{-1} \tag{6.18}$$

$$\phi_{s,M} = \omega_{\tilde{A}}\left[1+\frac{h^2}{2}+qhR_M\frac{\omega_{\tilde{K}}}{S_M+\omega_{\tilde{K}}}+\frac{q(q-1)}{2}R_M^2\left(\frac{\omega_{\tilde{K}}}{S_M+\omega_{\tilde{K}}}\right)^2\right] \times\left\{\omega_{\tilde{A}}\left[1+\frac{h^2}{2}+qhR_M\frac{\omega_{\tilde{K}}}{S_M+\omega_{\tilde{K}}} + \frac{q(q-1)}{2}R_M^2\left(\frac{\omega_{\tilde{K}}}{S_M+\omega_{\tilde{K}}}\right)^2\right]+\left(\frac{S_M+1}{S_M+\omega_{\tilde{K}}}\right)^q\right\}^{-1} \tag{6.19}$$

These results are equivalent to (3.9) if we consider the transcriptions (6.5) and also the result[2a,2b]

$$\phi_\mu = \tfrac{1}{2}\tilde{J}q\hat{e} + \tfrac{1}{2}hm \tag{6.20}$$

We conclude that both solutions of the equilibrium polymerization model on the Bethe lattice, the direct one and the one using the correspondence with the $n\to 0$ vector model, are identical in the whole $\tilde{J}$, h, $\tilde{K}$, $\tilde{A}$ parameter space. Thus, we do not observe in our solution any breakdown of the correspondence between the models, signaling the appearance of the "collapsed" phase recently suggested by Gujrati,[16,22] and there seems to be no reason to identify the polymerized phase obtained here with the "new" phase proposed in Ref. 16 as is suggested in Ref. 22.

It is interesting to notice that the following relation exists between our

results for the magnetization (6.17) in the thermodynamic limit and the density of polymers x_p in (3.9),

$$m = 2x_p/(2K_1)^{1/2} \tag{6.21}$$

A similar relation noted by Gujrati[22] in his solution of the equilibrium polymerization model on a Bethe lattice with $q = 3$ led him to propose a suitable definition for the order parameter of the equilibrium polymerization problem. Here we recover this result in a more general situation of arbitrary q and in the presence of a solvent, suggesting that the order parameter could be defined as the probability of having a polymer end at a particular site (i.e., $2x_p$) in the core of the tree (not necessarily the central site), divided by a statistical weight of a polymer end. [In Gujrati's[22] Eqs. (8) and (9) for this probability, κ must be replaced by $\kappa^{1/2}$ to get the correct result.]

In the limit of a pure $n \to 0$ vector model ($\omega_{\vec{A}} \to \infty$), the recursion relations will be given by (3.11) and the densities (6.17)–(6.19) are, in the thermodynamic limit, equal to

$$m = \frac{h + qR}{1 + \frac{1}{2}h^2 + qhR + \frac{1}{2}q(q-1)R^2} \tag{6.22}$$

$$\hat{e} = \frac{hR + (q-1)R^2}{\tilde{J}[1 + \frac{1}{2}h^2 + qhR + \frac{1}{2}q(q-1)R^2} \tag{6.23}$$

and

$$\phi_s = 1 \tag{6.24}$$

It is known[1a,1b] that, viewed as a magnetic model, the $n \to 0$ vector model exhibits regions of "thermodynamic instability," where the magnetic susceptibility becomes negative. In the mean-field approximation the region of positive susceptibility is a wedge-shaped region in the $\tilde{J}$, h plane containing the critical point and part of the coexistence curve. Recently we have shown[17] that nonclassical scaling equations of state obtained from the renormalization group via the ε expansion have a region of negative χ extending along the coexistence curve all the way to the critical point, and have suggested how this region may join with that of the mean-field approximation at high field. In one dimension[18] the region of negative χ is of still quite different shape, consisting of narrow wedges along the h axis through the critical point. It is therefore of some interest to obtain this region of negative χ for the Bethe-lattice solution, since this allows one to examine how the mean-field solution changes when correlations are introduced and see how the change to the one-dimensional behavior takes

place in the limit $q=2$. It should be emphasized, however, that the "instability" of the nonphysical magnet does not imply any corresponding instability of the corresponding polymer solution. All of the thermodynamic stability criteria are satisfied there, as discussed in Ref. 17.

For the sake of simplicity we will restrict ourselves to the $n \to 0$ vector model without dilution. The magnetization of this model is given in (6.22), whereas the fixed-point value R of the recursion relation (3.11) satisfies the equation

$$\tfrac{1}{2}(q-1)(q-2)R^3 + (q-1)hR^2 + [1 + \tfrac{1}{2}h^2 - \tilde{J}(q-1)]R - \tilde{J}h = 0 \tag{6.25}$$

The magnetic susceptibility is given by

$$\chi = \left(\frac{\partial m}{\partial h}\right)_{\tilde{J}} = \left(\frac{\partial m}{\partial h}\right)_{\tilde{J},R} + \left(\frac{\partial m}{\partial R}\right)_{\tilde{J},h}\left(\frac{\partial R}{\partial h}\right)_{\tilde{J}} \tag{6.26}$$

and the derivatives can be readily calculated using (6.22) and (6.25), yielding χ as a function of q, $\tilde{J}$, h, and R.

It is convenient to introduce the following reduced temperature for the magnetic model:

$$\tilde{\tau} = 1 - \tilde{T}_c/T = 1 - \tilde{J}/\tilde{J}_c = 1 - (q-1)\tilde{J} \tag{6.27}$$

Then the explicit expressions for the susceptibility on the $h=0$ axis become

$$\begin{aligned} \tilde{\tau} > 0: \quad & \chi(\tilde{\tau}, h=0) = \frac{q-\tilde{\tau}}{(q-1)\tilde{\tau}} \\ \tilde{\tau} < 0: \quad & \chi(\tilde{\tau}, h=0) = \frac{1}{[1-q\tilde{\tau}/(q-2)]^2}\left[1 + \frac{q(q+1)}{(q-1)(q-2)}\tilde{\tau}\right. \\ & \left. - \frac{q(q-2-q\tilde{\tau})^2}{2\tilde{\tau}(q-1)(q-2)^2}\right] \end{aligned} \tag{6.28}$$

The susceptibility on the $h=0$ axis is therefore always positive for $\tilde{\tau} > 0$, but it will be negative in some regions of the $\tilde{\tau} < 0$ semiaxis. The points on the $h=0$, $\tilde{\tau} < 0$ semiaxis where the susceptibility vanishes are the negative values of the expression

$$\begin{aligned} \tilde{\tau}_0 = & \frac{(6q-4)(q-2)}{4q(q+1)(q-2) - 2q^3} \\ & \times \left\{1 \pm \left[1 + \frac{4q(q-2)[2q(q+1) - q^3/(q-2)]}{(6q-4)^2}\right]^{1/2}\right\} \end{aligned} \tag{6.29}$$

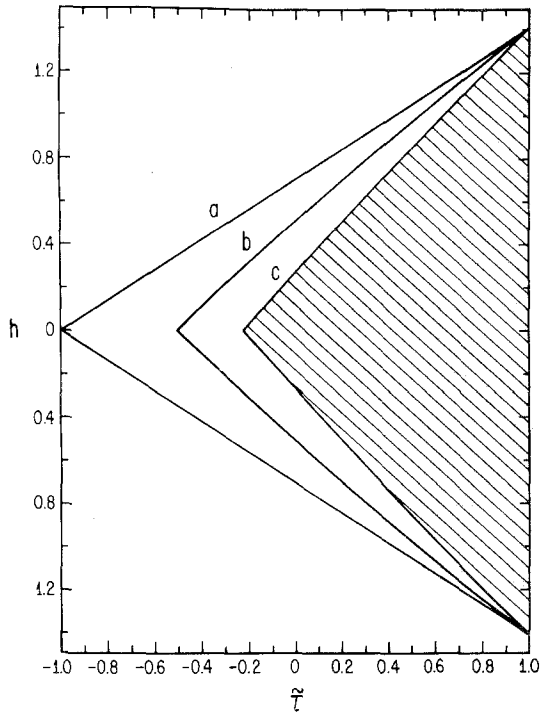

Fig. 8. Zero-susceptibility curves in the $\tilde{\tau} = 1 - T_c/T$, h space for the Bethe lattice solution for $n \to 0$ vector model without dilution. The curves shown are (a) $q \to \infty$ (mean field), (b) $q = 6$, and (c) $q = 3$. The hatched region comprises points of positive susceptibility for the model with $q = 3$.

For $q < 1 + \frac{1}{2}\sqrt{20} = 3.2360...$ there are two negative values for $\tilde{\tau}_0$, and χ changes sign twice, being positive at very low temperatures. In Fig 8 the $\chi = 0$ curves are depicted for $q \to \infty$, $q = 6$, and $q = 3$. In the mean-field limit $q \to \infty$ they are straight lines $h = \pm 2^{-1/2}(\tilde{\tau} + 1)$; for $q = 6$ and $q = 3$ the curves are slightly curved. That the value of τ at which $\chi(h = 0)$ changes sign becomes less negative as correlations are included is consistent with a recent conjecture[17] concerning the shape of the $\chi = 0$ curves for the $n \to 0$ vector model when both fluctuations and corrections to scaling are taken into account. The $\chi > 0$ region for $q = 3$ is hatched in the figure. It should be noted that for $q = 3$ there is another region of positive susceptibility for $\tilde{\tau} < -4.44152...$ which is outside the range of values for $\tilde{\tau}$ in Fig. 8.

In Fig. 9 (curve a), we present the zero-susceptibility curves for the one-dimensional $n \to 0$ vector model without dilution. The susceptibility in this case may be calculated similarly to the calculation above, by setting

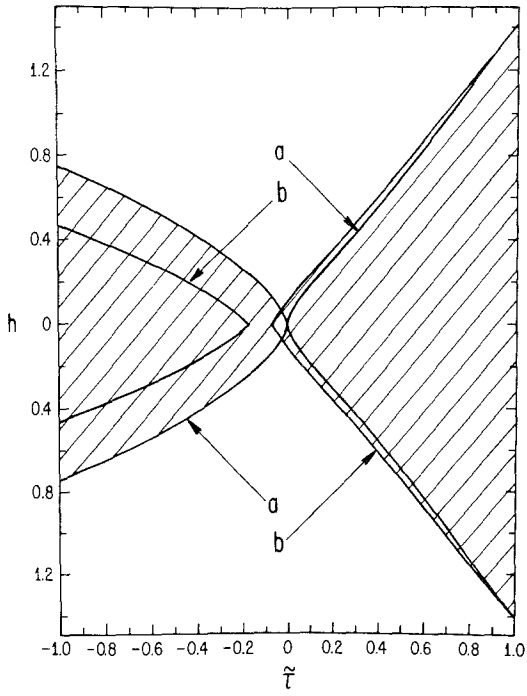

Fig. 9. (a) Zero-susceptibility curves in the $\tilde{\tau}$, h space for the one-dimensional ($q=2$) $b \to 0$ vector model without dilution. In the hatched region the susceptibility is positive. (b) The curves of zero susceptibility for the model with $q=2.2$.

$q=2$ in expressions (6.22) for the magnetization and in the equation (6.25) for the fixed-point values of R. The general expressions for the susceptibility of the one-dimensional model are too lengthly to be included here, but for $h=0$ they reduce to

$$\begin{aligned} \tilde{\tau}>0: &\qquad \chi(\tilde{\tau}, h=0)=(2-\tilde{\tau})/\tilde{\tau} \\ \tilde{\tau}<0: &\qquad \chi(\tilde{\tau}, h=0)=-2/\tilde{\tau} \end{aligned} \tag{6.30}$$

[The expressions for the susceptibility on the $h=0$, $\tilde{\tau}<0$ semiaxis in Eqs. (3.20) and (3.43) of Ref. 14 contain an error: the numerator $2\tilde{J}$ should be replaced by 2.] Expressions (6.30) show that the susceptibility for $q=2$ is always nonnegative on the $h=0$ axis; the regions of negative susceptibility are located at nonzero magnetic field. As an illustration, we show in Fig. 9 the curves of zero susceptibility for a model with $q=2.2$, showing the two regions of positive susceptibility quite close to each other.

It should be stressed that, to study the one-dimensional model, one must take $q=2$ before setting $h=0$, since different results may be obtained

if the limit $q \to 2$ is taken in the final expression for the thermodynamic quantities for general q. In particular we note that

$$\lim_{q \to 2} \lim_{h \to 0^+} \chi(q\tilde{\tau}, h; q) = -1/\tilde{\tau} \tag{6.31}$$

when $\tilde{\tau} < 0$, which is different from the one-dimensional result (6.30). The limits $q \to 2$ and $h \to 0$ are not interchangeable for $\tilde{\tau} < 0$. The delicacy of this limit is apparent already in Eq. (6.25) for R. For $q > 2$ the limit $h \to 0$ implies $R \to 0$ for $\tau \geqslant 0$, which in turn implies that m in Eq. (6.22) tends to 0. For $\tau < 0$, Eq. (6.25) admits the solution $R = \pm[-2\tau/(q-1)(q-2)]^{1/2}$ as $h \to 0$ for $q > 2$, which leads to $m \sim (-2\tau)^{1/2}$ for $\tau < 0$ and $h = 0$, and to $m(h \to 0,\ \tau < 0) \to 0$ as $1 \to 2$. However, if the limit $q \to 2$ is taken for Eq. (25) before $h \to 0$, then the limit $h \to 0$ gives $R = 0$ for both $\tau > 0$ and $\tau < 0$, but yields $R \to \pm[J/(q-1)]^{1/2}$ as $h \to 0$ with $\tau = 0$. This in turn gives the correct limit in one dimension $m(h \to 0^+,\ \tau = 0) = 1$.

7. DISCUSSION

The model proposed by Wheeler and Pfeuty[2a,2b] for equilibrium polymerization in solution is solved exactly on the Bethe lattice with coordination number q. Although the solution is direct, we also show that the solution of an equivalent dilute $n \to 0$ vector model on the Bethe lattice leads to the same results. The Bethe-lattice solution becomes identical to the mean-field results in the limit of infinite coordination number ($q \to \infty$) and to the solution of the one-dimensional model when $q = 2$. Phase diagrams for finite $q > 2$ show differences, indicating increased cooperativity when compared with the ones obtained by the mean-field approach, although the exponents remain classical.

Although the Bethe-lattice solution displays classical critical exponents, it should be stressed that first-neighbor correlations are treated exactly in the Bethe–Peierls approximation. This is of some significance for the equilibrium polymerization problem since the magnetic first-neighbor spin–spin correlations are directly related to the density of monomers incorporated into polymers ϕ_μ [see expression (6.20)].

The method presented by Gujrati[22] for $q = 3$ can, in principle, be generalized for any q, but for each new value of q a separate underlying Ising model has to be considered, so that the procedure is unnecessarily tedious for general q. The method presented here has the advantage that it proceeds naturally and straightforwardly for any q, with q as a parameter in the theory, thus facilitating direct comparisons in the one-dimensional ($q = 2$) and mean-field ($q \to \infty$) limits.

APPENDIX A. ONE-DIMENSIONAL LIMIT

The recursion relations (3.5) and densities (3.9) of the solution of the model on the Bethe lattice become, for $q=2$,

$$R_{M+1}=\frac{(2K_1)^{1/2}K_p'[S_M+\omega_{\bar{K}}]+\omega_{\bar{K}}K_p'R_M}{(1+K_1)[S_M+\omega_{\bar{K}}]+\omega_{\bar{K}}(2K_1)^{1/2}R_M}$$
$$S_{M+1}=\frac{S_M+1}{\omega_{\bar{A}}\{(1+K_1)[S_M+\omega_{\bar{K}}]+\omega_{\bar{K}}(2K_1)^{1/2}R_M\}} \tag{A.1}$$

and

$$\begin{aligned}
x_{m,M}&=1-[S_M+1]^2\\
&\quad\times([S_M+1]^2+\omega_{\bar{A}}\{(1+K_1)[S_M+\omega_{\bar{K}}]^2\\
&\quad+2(2K_1)^{1/2}\omega_{\bar{K}}R_M[S_M+\omega_{\bar{K}}]+\omega_{\bar{K}}^2R_M^2\})^{-1}\\
x_{p,M}&=\omega_{\bar{A}}\{K_1[S_M+\omega_{\bar{K}}]^2+(2K_1)^{1/2}\omega_{\bar{K}}R_M[S_M+\omega_{\bar{K}}]\}\\
&\quad\times([S_M+1]^2+\omega_{\bar{A}}\{(1+K_1)[S_M+\omega_{\bar{K}}]^2\\
&\quad+2(2K_1)^{1/2}\omega_{\bar{K}}R_M[S_M+\omega_{\bar{K}}]+\omega_{\bar{K}}^2R_M^2\})^{-1}\\
x_{b,M}&=\omega_{\bar{A}}\{(2K_1)^{1/2}\omega_{\bar{K}}R_M[S_M+\omega_{\bar{K}}]+\omega_{\bar{K}}^2R_M^2\}\\
&\quad\times([S_M+1]^2+\omega_{\bar{A}}\{(1+K_1)[S_M+\omega_{\bar{K}}]^2\\
&\quad+2(2K_1)^{1/2}\omega_{\bar{K}}R_M[S_M+\omega_{\bar{K}}]+\omega_{\bar{K}}^2R_M^2\})^{-1}
\end{aligned} \tag{A.2}$$

In the pure solute limit $\omega_{\bar{A}}\to\infty$, the one-dimensional equilibrium polymerization results[18] are recovered. In the particular case $K_1=0$ the recursion relations reduce to

$$R_{M+1}=\frac{\omega_{\bar{K}}K_p'}{S_M+\omega_{\bar{K}}}R_M,\qquad S_{M+1}=\frac{1}{\omega_{\bar{A}}}\frac{S_M+1}{S_M+\omega_{\bar{K}}} \tag{A.3}$$

We notice that the step-function behavior already present in the pure monomer case[18] happens also when solvent is present. The recursion relation for R will have two fixed points, $R=0$ (unpolymerized) and $R=\infty$ (polymerized). The unpolymerized fixed point will be attained whenever

$$\omega_{\bar{K}}K_p/(S+\omega_{\bar{K}})<1 \tag{A.4}$$

and a first-order transition to a phase with $\phi_\mu=1$ occurs when the coefficient equals unity. Since, at the fixed point

$$S=\frac{(1-\omega_{\bar{A}}\omega_{\bar{K}})\pm[(1-\omega_{\bar{A}}\omega_{\bar{K}})^2+4\omega_{\bar{A}}]^{1/2}}{2\omega_{\bar{A}}}\geqslant 0 \tag{A.5}$$

the phase transition happens for $K_p' \geqslant 1$, the equality being valid for the pure solute limit.

APPENDIX B. DERIVATION OF THE MEAN-FIELD FREE ENERGY

We show in this Appendix how the free energy can be obtained from the man-field fixed-point conditions (3.22). For $h=0$, these conditions are

$$m = \frac{q\tilde{J}m\omega_{\tilde{\Delta}} \exp(qKx_s)}{1+[1+\frac{1}{2}(q\tilde{J}m)^2]\omega_{\tilde{\Delta}} \exp(qKx_s)} \tag{B.1}$$

$$(1-x_s)^{-1} = 1+\omega_{\tilde{\Delta}} \exp(qKx_s)[1+\tfrac{1}{2}(q\tilde{J}m)^2]$$

The solutions may be found in two branches

$$m=0: \qquad \omega_{\tilde{\Delta}_0} = \frac{x_s}{(1-x_s)\exp(qKx_s)} \tag{B.2}$$

$$m\neq 0: \qquad \omega_{\tilde{\Delta}_1} = \frac{1}{(1-x_s)\, q\tilde{J} \exp(qKx_s)} \tag{B.3}$$

Now, since we have for the free energy $g(\tau, x_s)$ the relation

$$\tilde{\Delta} = (\partial g/\partial x_s)_{\tilde{\tau}} \tag{B.4}$$

it is possible to obtain the free energies of the two branches by integrating over the fields,

$$\begin{aligned} g_0 &= \int \tilde{\Delta}_0 \, dx_s = -\tfrac{1}{2}qKx_s^2 + x_s \ln x_s + (1-x_s + (1-x_s)\ln(1-x_s) + C_0 \\ g_1 &= \int \tilde{\Delta}_1 \, dx_s = -\tfrac{1}{2}qKx_s^2 - x_s(\ln q\tilde{J} - 1) + (1-x_s)\ln(1-x_s) + C_1 \end{aligned} \tag{B.5}$$

where C_0 and C_1 are arbitrary functions of $\tilde{\tau}$ only. The Legendre transforms of these free energies

$$f_{0,1}(\tilde{\tau}, \tilde{\Delta}) = g_{0,1}(\tilde{\tau}, x_s) - \tilde{\Delta}_{0,1} x_s$$

are

$$\begin{aligned} f_0 &= \tfrac{1}{2}qKx_s^2 + \ln(1-x_s) + C_0 \\ f_1 &= \tfrac{1}{2}qKx_s^2 + x_s + \ln(1-x_s) - C_1 \end{aligned} \tag{B.6}$$

Now the polymerized ($m \neq 0$) and unpolymerized regions merge continuously at the critical line, which is given by

$$\omega_{\tilde{A}_0} = \omega_{\tilde{A}_1} \to q\tilde{J}x_s = 1 \tag{B.7}$$

and, arbitrarily fixing $C_0 = 0$, by imposing continuity of the free energy at the critical line, we obtain

$$\begin{aligned} f_0 &= \tfrac{1}{2}qKx_s^2 + \ln(1 + x_s) \\ f_1 &= \tfrac{1}{2}qKx_s^2 + (x_s - 1/q\tilde{J}) + \ln(1 - x_s) \end{aligned} \tag{B.8}$$

Now, from (B.1) we notice that, for $m \neq 0$,

$$\tfrac{1}{2}q\tilde{J}m^2 = x_s - 1/q\tilde{J} \tag{B.9}$$

allowing us to rewrite f_1 as follows:

$$f_1 = \tfrac{1}{2}qKx_s^2 + \tfrac{1}{2}q\tilde{J}m^2 + \ln(1 - x_s) \tag{B.10}$$

which correspond to the mean-field result (5.17) in the paper by Wheeler and Pfeuty.[2b]

ACKNOWLEDGMENTS

This research was supported by the NSF through grant CHE 81-10247. One of us (J.E.S.) acknowledges a travel grant by CAPES (Brazil).

REFERENCES

1a. J. C. Wheeler, S. J. Kennedy, and P. Pfeuty, *Phys. Rev. Lett.* **45**:1784 (1980).
1b. J. C. Wheeler and P. Pfeuty, *Phys. Rev. A* **24**:1050 (1981).
2a. J. C. Wheeler and P. Pfeuty, *Phys. Rev. Lett.* **46**:1409 (1981).
2b. J. C. Wheeler and P. Pfeuty, *J. Chem. Phys.* **74**:6415 (1981).
3. P. G. De Gennes, *Phys. Lett.* **38A**:349 (1972).
4. J. Des Cloizeaux, *J. Phys.* **36**:281 (1972).
5. G. Gee, *Trans. Faraday Soc.* **48**:515 (1982).
6. A. V. Tobolsky and A. Eisenberg, *J. Am. Chem. Soc.* **81**:780 (1959).
7. R. L. Scott, *J. Phys. Chem.* **69**:261 (1965).
8. S. J. Kennedy and J. C. Wheeler, *J. Phys. Chem.* **85**:1040 (1984).
9. S. J. Kennedy and J. C. Wheeler, *J. Chem. Phys.* **78**:1523 (1983).
10. S. Greer, *J. Chem. Phys.* **84**:6984 (1986).
11. S. J. Kennedy and J. C. Wheeler, *J. Chem. Phys.* **78**:953 (1983).
12. C. M. Knobler and R. L. Scott, in *Phase Transitions and Critical Phenomena*, Vol. 9, C. Domb and J. L. Lebowitz, eds. (Academic Press, New York, 1984).
13. E. Müller-Hartmann and J. Zittartz, *Phys. Rev. Lett.* **33**:893 (1974).

14. T. P. Eggarter, *Phys. Rev. B* **9**:2989 (1974).
15. R. J. Baxter, *Exactly Solved Models in Statistical Mechanics* (Academic Press, London, 1982).
16. P. D. Gujrati, *Phys. Rev. B* **31**:4375 (1985); P. Gujrati, *Phys. Rev. Lett.* **55**:1161 (1985).
17. J. C. Wheeler, J. F. Stilck, R. G. Petschek, and P. Pfeuty, *Phys. Rev. B* **35**:284 (1987).
18. P. M. Pfeuty and J. C. Wheeler, *Phys. Rev. A* **27**:2178 (1983).
19. C. J. Thompson, *J. Stat. Phys.* **27**:441 (1982).
20. M. J. de Oliveira and S. R. Salinas, *Rev. Bras. Fiš.* **15**:189 (1985).
21. C. S. O. Yokoi, M. J. de Oliveira, and S. R. Salinas, *Phys. Rev. Lett.* **54**:163 (1985).
22. P. D. Gujrati, *Phys. Rev. Lett.* **53**:2453 (1984).
23. S. Muto and T. Oguchi, *Prog. Theor. Phys.* **55**:81 (1976).
24. P. D. Gujrati, *Phys. Rev. A* **24**:2096 (1981).
25. R. L. Scott, in *Elemental Sulfur*, B. Meyer, ed. (Wiley, New York, 1965).
26. J. C. Wheeler and L. R. Corrales, in preparation.